The Transition from Free to Ambipolar Diffusion*

W. P. ALLIS, *Research Laboratory of Electronics, Massachusetts Institute of Technology, Cambridge, Massachusetts*

AND

D. J. ROSE, *Bell Telephone Laboratories, Murray Hill, New Jersey*

(Received September 30, 1953)

In gas discharge plasmas with very low charge densities, the charged particles diffuse freely in directions perpendicular to the applied electric field because the space-charge field is negligible. At high charge densities, the space-charge field saturates and gives rise to a combination of diffusive and mobility flow termed ambipolar. The transition between these limits is examined theoretically for the case of plasmas maintained through ionization by electron impact. The ionization frequency per electron, one of the principal parameters of the transition, can be re-expressed in terms of an effective diffusion coefficient; it falls from a high value at the free diffusion limit to a low value at the ambipolar limit as the electron density increases over many orders of magnitude. The transition is accompanied by changes in the charge distributions and by the development of a positive ion sheath. The current equations determining the process are examined, and approximate solutions are obtained. Second approximations are obtained for the case where the ratio of electron to ion energies is much greater than unity. Machine solutions are presented both for the above case and for an isothermal plasma in which this ratio equals unity. An application to the afterglow is shown.

I. INTRODUCTION

THIS paper deals with the spatial distributions of the charged particles, space-charge fields, and voltages in certain types of gas discharge plasmas and with the rate of ionization necessary to maintain the plasma in a steady state. Specifically the problem to be investigated is as follows: the electrons and ions created by electron collision tend to diffuse out of the plasma, and, since the electrons are faster, a positive excess develops. Thus a space-charge field is built up which assists the ion and retards the electron currents. In the steady state, the two currents are equal. At the same time, each electron must have, on the average, one ionizing collision in the plasma before escaping in order to maintain the steady state. Since the space charge field reduces the electron escape rate it also reduces the required ionization rate per electron per second. This ionization frequency is one of the fundamental parameters of the plasma; it is large at low densities where the space-charge field is small and smaller at high densities.

The limiting cases of very low charge density (free diffusion) and very high density (ambipolar diffusion) are well known. The transition between them involves nonlinear processes and has not been investigated in sufficient detail. The present paper describes this transition as it occurs in certain simple plasmas; expressions will be derived for the ionization rate, charge densities, space-charge field, and other quantities; and the nature of the plasma sheath will be discussed.

We state the basic definitions and assumptions: (1) the plasma contains electrons and ions in concentrations N and P respectively; (2) these charges are produced by collisions at the rate νN per unit volume, where ν is the frequency of ionization by an electron; (3) the pressure of neutral gas is sufficiently high for the mean free paths to be small compared to all relevant dimensions. The mean motions of the charged particles will then be determined by diffusion and mobility, with coefficients D_-, D_+, μ_-, μ_+; (4) the applied electric field does *not* accelerate the charged particles toward the walls, but the space charge field $\mathbf{E}$ will in general draw the ions toward the walls and repel the electrons; (5) the electrons and ions stick to the walls when they reach them and recombine there, there being no volume recombination or attachment; (6) for mathematical simplicity it is assumed that the mean energy of each kind of particle is uniform throughout the plasma so that all the coefficients are constants. The ratio D_-/μ_- is approximately equal to k_0T_-/e, where k_0 is Boltzmann's constant, T_- the electron temperature, and e the electronic charge. D_-/μ_- is very close to two-thirds of the potential corresponding to the average electron energy in electron volts and similarly for D_+/μ_+ and the energy of the ions. The above conditions are substantially satisfied in high-frequency electrical discharges and in the positive column of dc discharges; in both of these cases $D_-\mu_+/D_+\mu_-\gg 1$. Such discharges will be called active plasmas. The theory presented also applies in part to cases in which this ratio has less extreme values, and in particular to an isothermal plasma where $D_-/\mu_-=D_+/\mu_+$; this latter situation occurs in a decaying plasma.

Because of mathematical complexity the solutions obtained are in general not exact. An approximate solution to the general case is found and upper and lower bounds are found for certain parameters. Machine solutions are also obtained for both active and isothermal plasmas, and a better analytic approximation is derived for the active case; but the authors have not found a converging series of approximations for the general case.

* This work has been supported in part by the U. S. Army Signal Corps, the U. S. Air Materiel Command, and the U. S. Office of Naval Research.

II. BASIC EQUATIONS

The particle current $\mathbf{\Gamma}$ per unit area for the electrons is

$$\mathbf{\Gamma}=-D_-\nabla N-\mu_-\mathbf{E}N, \tag{1}$$

and for the positive ions

$$\mathbf{\Gamma}=-D_+\nabla P+\mu_+\mathbf{E}P. \tag{2}$$

In the steady state these two flows are equal; thus from the assumption regarding the production of charges,

$$\nabla\cdot\mathbf{\Gamma}=N\nu. \tag{3}$$

Finally, Poisson's equation

$$\nabla\cdot\mathbf{E}=e(P-N)/\epsilon_0 \tag{4}$$

must hold, where $e/\epsilon_0=1.809\times10^{-8}$ volt-meter.

In an isothermal afterglow, the electron and ion currents are not necessarily equal, and since there is no ionization, (3) is replaced by

$$\nabla\cdot\mathbf{\Gamma}=-\partial N/\partial t. \tag{3a}$$

However, it will be shown later that in such cases the density decays almost exponentially over the principal range of interest, so that $\partial N/\partial t$ is very nearly proportional to N, and the two currents are approximately equal. Thus in an afterglow, $-\nu$ is to be interpreted as the decay rate.

These equations will be solved subject to the boundary condition

$$P_1=N_1=0 \tag{5}$$

at the walls. Strictly, these quantities are not quite zero but vanish at extrapolated points outside the walls, and the extrapolation is greater for the ions than for the electrons due to the effect of the electric field. However the difference may be made small by decreasing the mean free path, and it will be assumed that the pressure is sufficiently high for the boundary condition (5) to be used.

The theory applies to symmetrical geometries so that there is a central point at which $\mathbf{\Gamma}=\mathbf{E}=0$, and this will be chosen as the origin of coordinates. It will be seen that there is a relation between the central concentrations N_0 and P_0, leaving only one of them arbitrary. We shall choose N_0 as the independent parameter because it is the principal factor in the conductivity of the plasma, and this is the quantity which is generally measured.

III. CONSTANT RATIO APPROXIMATION

At very low densities, for example at breakdown, the space charge field $\mathbf{E}$ may be neglected. Equations (1) and (3) then give the well-known diffusion equation

$$D_-\nabla^2N+\nu N=0. \tag{6}$$

The boundary condition (5) converts this into a characteristic value problem: one can define a diffusion length Λ for any shaped cavity (strictly a set of diffusion lengths Λ_i, but only the largest is of interest to us), and (6) has no solution satisfying (5) unless

$$\nu=D_-/\Lambda^2. \tag{7}$$

As the ionization frequency ν is in general a function of the applied field, this is the equation which determines the field at which breakdown occurs: it is the field for which the ionization rate $N\nu$ equals the diffusion rate ND_-/Λ^2.

The positive ion distribution is then found by solving for $\mathbf{\Gamma}$ and substituting in Eq. (2). The result may be expressed in terms of the ratio P/N:

$$r=P/N=D_-/D_+. \tag{8}$$

The positive ion concentration is much higher than the electron concentration so that the positive ion diffusion rate PD_+/Λ^2 equals the electron diffusion rate. It is our purpose to generalize Eqs. (7) and (8) to apply when space charge is effective.

The excess ion concentration produces a space charge whose field retards the electrons and accelerates the ion flow towards the walls, thus decreasing both ν and r. The form of Eq. (7) can be preserved by defining an effective diffusion coefficient

$$D_s=\nu\Lambda^2, \tag{9}$$

whereupon the problem is reduced to that of expressing D_s in terms of N_0 and the diffusion and mobility coefficients. D_s will decrease with increasing N_0, and this is the origin of the negative characteristic of a glow discharge at low currents.

The unknown space-charge field $\mathbf{E}$ can be eliminated between Eqs. (1) and (2) to give

$$\mathbf{\Gamma}=-\frac{\mu_+D_-P\nabla N+\mu_-D_+N\nabla P}{\mu_+P+\mu_-N}; \tag{10}$$

and if we make the naive assumption that the ratio r is independent of position this yields

$$\mathbf{\Gamma}=-\frac{\mu_+D_-+\mu_-D_+}{\mu_+r+\mu_-}r\nabla N=-D_r\nabla N. \tag{11}$$

The above procedure is that generally used[1] to derive the ambipolar diffusion coefficient

$$D_a=\frac{\mu_+D_-+\mu_-D_+}{\mu_++\mu_-}, \tag{12}$$

which applies in the high-current limit when $r=1$. The expression for D_r also reduces to D_- in the low-current limit when $r=D_-/D_+$. It will be shown that in the intermediate range the ratio r is not independent of position and the expression for D_r is too small ($D_r<D_s$). Nevertheless the expression for D_r is a convenient approximation to D_s, which will be called the constant ratio approximation (c.r.a.).

[1] A. von Engel and M. Steenbeck, *Elektrische Gasentladungen* (Edwards Brothers, Inc., Ann Arbor, 1944), Vol. 1, p. 199.

Introducing the constant ratio assumption into Eqs. (3) and (4) leads to the relation

$$e(P_0-N_0)/\epsilon_0\nu=(D_-/r-D_+)/(\mu_+D_-+\mu_-D_+), \quad (13)$$

by which the ratio r can be determined, to this approximation, in terms of the central space charge $e(P_0-N_0)$.

As Eqs. (11) and (13) are not exact, it is convenient to have an upper limit on the central space charge. This is found by requiring that the positive ion concentration by a maximum at the center; thus

$$(\nabla^2 P)_0<0,$$

whence

$$\nu N_0=(\boldsymbol{\nabla}\cdot\boldsymbol{\Gamma})_0=(\mu_+P\boldsymbol{\nabla}\cdot\mathbf{E}-D_+\nabla^2P)_0 > e\mu_+P_0(P_0-N_0)/\epsilon_0$$

or

$$1/r_0>\mu_+e(P_0-N_0)/\epsilon_0\nu. \quad (14)$$

This relation will be called the central maximum bound.

IV. THE ELECTRON AND ION DEBYE LENGTHS

Debye and Hückel[2] have introduced a distance λ_D at which the ions in an electrolyte will shield any stationary charge:

$$\frac{1}{\lambda_D^2}=\frac{\epsilon_0e^2}{k_0}\left(\frac{P}{T_+}+\frac{N}{T_-}\right). \quad (15)$$

In an electrolyte the two quantities in parentheses are equal. In a plasma they are far different, and we must introduce two quantities,

$$\lambda_n^2=\epsilon_0D_-/Ne\mu_-, \quad (16)$$

$$\lambda_p^2=\epsilon_0D_+/Pe\mu_+, \quad (17)$$

representing the shielding distances by the electrons and ions, respectively. The two distances are equal only for an isothermal plasma at the ambipolar limit.

Adopting the constant ratio approximation, one has at the center

$$\left(\frac{\Lambda}{\lambda_n}\right)^2\geq\frac{n_0(D_--D_r)}{s_0D_-}=\left(\frac{D_--D_r}{D_-}\right)^2\frac{D_a}{D_--D_a}. \quad (18)$$

Thus it is principally the electron shielding distance λ_n which controls the transition to ambipolar diffusion and when $\lambda_n=\Lambda$ the ion density is about twice the electron density and $D_r\approx2D_a$. This is about midway in the transition.

The Debye lengths also figure in the development of the sheath. The wall strongly affects the electron density within the distance λ_n of the wall and the ion density within the distance λ_p. In an active plasma, $\lambda_n\gg\lambda_p$; the positive ion sheath is in reality an electron deficiency, and its thickness is closely related to λ_n. On the outside of the sheath there is a thin region whose thickness is of the order λ_p and whose potential is of the order D_+/μ_+, in which the ion density adjusts to meet the boundary condition. We shall term this region the "skin." This skin becomes infinitely thin as $D_+\mu_-/D_-\mu_+\to0$; or, in physical terms, if $D_+=0$, the ions have no random motion, and then the absorption of the ions by the walls can have no effect on their density inside the plasma.

In an isothermal plasma, on the other hand, $\lambda_p\approx\lambda_n$ at densities high enough to form a well-developed sheath. Thus the sheath and skin become indistinguishable, and perturbations in the ion boundary condition can be transmitted through the sheath into the plasma. The consequences of this latter situation will be illustrated in Sec. VIII.

[2] P. Debye and E. Hückel, Physik. Z. 24, 190 (1923).

V. DIMENSIONLESS VARIABLES

The number of independent parameters can be reduced to the following two:

$$\sigma=\mu_-/\mu_+, \quad \rho=\mu_-D_+/\mu_+D_-, \quad (19)$$

where ρ is the ratio of ion energy to electron energy. This quantity is therefore 1 in an isothermal plasma but is of the order 1/100 for an active plasma.

Consider the dimensionless variables

$$n=Ne\mu_+/\epsilon_0\nu; \quad s=(P-N)e\mu_+/\epsilon_0\nu; \quad (20)$$

$$\mathbf{G}=\boldsymbol{\Gamma}e\mu_+/\epsilon_0\nu(D_-\nu)^{\frac{1}{2}}; \quad \mathbf{H}=\mathbf{E}\mu_+/(D_-\nu)^{\frac{1}{2}}; \quad (21)$$

$$\xi=x(\nu/D_-)^{\frac{1}{2}}, \quad (22)$$

where x stands for any linear coordinate. The Debye lengths are related to these transformations as follows:

$$n\xi^2=(\mu_+/\mu_-)(x/\lambda_n)^2, \qquad (n+s)\xi^2=(D_+/D_-)(x/\lambda_p)^2. \quad (23)$$

In terms of the dimensionless variables the basic equations (1)–(4) become

$$\boldsymbol{\nabla}n+\mathbf{G}=-\sigma\mathbf{H}n; \quad (24)$$

$$(1+\rho)\boldsymbol{\nabla}n+(1+\sigma)\mathbf{G}=\sigma\mathbf{H}s-\rho\boldsymbol{\nabla}s; \quad (25)$$

$$\boldsymbol{\nabla}\cdot\mathbf{G}=n; \quad \boldsymbol{\nabla}\cdot\mathbf{H}=s; \quad (26)$$

with the boundary condition

$$n_1=s_1=0 \quad (27)$$

at ξ_1, the wall. By eliminating n and s one obtains the two second-order, second-degree equations

$$\nabla^2\mathbf{G}+\mathbf{G}=-\sigma\mathbf{H}\boldsymbol{\nabla}\cdot\mathbf{G}, \quad (24a)$$

$$(1+\rho)\nabla^2\mathbf{G}+(1+\sigma)\mathbf{G}=\sigma\mathbf{H}\boldsymbol{\nabla}\cdot\mathbf{H}-\rho\nabla^2\mathbf{H}. \quad (25a)$$

The characteristic value parameter ν has vanished from these equations but occurs in the scale factor. The problem now is to find pairs of central values, (n_0, s_0), which yield solutions of (24) and (25) satisfying (27) for the same value, ξ_1, of the coordinates. The value of ν is then obtained by fitting ξ_1 to the known wall coordinate x_1, and the effective diffusion coefficient is

given by

$$D_s = D_-(\Lambda\xi_1/x_1)^2. \tag{28}$$

It is measured by the value of ξ_1 and a geometrical factor x_1/Λ characteristic of the volume containing the plasma. For parallel planes, $x_1/\Lambda=\pi/2$; for a long cylinder, $x_1/\Lambda=2.405$; for a sphere, $x_1/\Lambda=\pi$.

The nature of the free and ambipolar limits is well illustrated by Eqs. (24) and (25). In the free limit the effect of the space charge field is negligible, therefore we neglect the field $\mathbf{H}$ but keep the space charge s itself which is, in fact, large compared to n. After taking divergences, we have

$$\begin{aligned} &\nabla^2 n + n = 0, \\ &\rho s = (\sigma-\rho)n. \end{aligned} \tag{29}$$

On the other hand, in the ambipolar limit both $\mathbf{H}$ and s saturate, but n and $\mathbf{G}$ do not, so that we may neglect the right-hand side of (25), obtaining

$$\begin{aligned} &(1+\rho)\nabla^2 n + (1+\sigma)n = 0, \\ &\mathbf{H} = (\sigma-\rho)\mathbf{G}/(1+\rho)\sigma n, \\ &s = \frac{\sigma-\rho}{\sigma(1+\rho)}\left(1+\frac{1+\sigma}{1+\rho}\frac{G^2}{n^2}\right). \end{aligned} \tag{30}$$

In the ambipolar limit the space charge reaches a saturation value given by

$$s_a = (\sigma-\rho)/\sigma(1+\rho) \tag{31}$$

at the center and becomes infinite near the walls. The assumption $s \ll n$ is therefore necessarily false near the walls, and the ambipolar solution, defined by (30), is approached as n increases only in the sense that the region near the walls in which $s > n$, and which constitutes the positive ion sheath, becomes smaller as n increases. It should be noted also that the space-charge distribution is quite different in the two limits. For parallel planes, $n(\xi)$ is a cosine function in both limits. s is also a cosine in the free limit but is a secant squared in the ambipolar limit.

VI. APPROXIMATIONS AND LIMITS

An alternate and more useful form of the constant ratio approximation is found from the dimensionless equations by adding $\sigma\mathbf{G}s_0$ to both sides of (24a) and taking the divergence:

$$\nabla^2 n + k^2 n = \sigma\boldsymbol{\nabla}\cdot(\mathbf{G}s_0 - \mathbf{H}n) \approx 0, \tag{24b}$$

where

$$k^2 = 1+\sigma s_0. \tag{32}$$

Since s_0 is the central value of s, it is seen that the right-hand side of (24b) and its first derivative vanish at the center; and therefore a relatively small error is made in neglecting it. The equivalence of the approximate form of (24b) and the previous form of the constant ratio approximation (11) depend on assuming a relation between s_0 and r which is

$$\sigma s_0 = (\sigma - r\rho)/r(1+\rho). \tag{33}$$

Such a relation is equivalent to setting $\nabla^2 N/N = \nabla^2 P/P$ at the center—that is, to forcing both charge distributions to have the same shape near the center.

In the approximation (24b), n is a solution of the diffusion equation for a cavity of diffusion length $1/k$. As the right-hand side of the equation is positive, the electrons actually assume a bell-shaped distribution, the appearance of which indicates the formation of the sheath. Thus the distribution of n is no longer everywhere convex, and the concentration actually extends beyond that predicted by the approximation. Thus $D_r = D_-/k^2$, and we have the inequality

$$D_s \geq D_-/k^2. \tag{34}$$

The equality holds both in the free limit for $s_0=0$ and in the ambipolar limit where

$$D_a = D_-(1+\rho)/(1+\sigma) \tag{35}$$

for $s_0 = s_a$. It will be shown below that between these limits the effective diffusion coefficient D_r calculated by this formula may be too small by a factor as large as 3.

The central ratio n_0/s_0 is obtained by dividing (25) by $\sigma\mathbf{H}$ and seeking the limit of each term at the center. In particular $(\mathbf{G}/\mathbf{H})_0 = n_0/s_0$. In this way one obtains

$$(1+\rho)(s_a - s_0)n_0/s_0 = s_0 - (\rho/\sigma)(\nabla^2\mathbf{H}/\mathbf{H})_0. \tag{36}$$

The ratio $(\nabla^2\mathbf{H}/\mathbf{H})_0$ cannot be determined without reference to the boundary conditions. However it is noted that near the free limit (29)

$$\nabla^2\mathbf{H}/\mathbf{H} = \nabla^2\mathbf{G}/\mathbf{G} = -k^2;$$

whereas near the ambipolar limit (30)

$$\begin{aligned} \nabla^2\mathbf{H}/\mathbf{H} = (n/\mathbf{G})\nabla^2(\mathbf{G}/n) = (n/\mathbf{G})\boldsymbol{\nabla}[1+(kG/n)^2] \\ = 2k^2\boldsymbol{\nabla}\cdot(\mathbf{G}/n), \end{aligned}$$

so that $(\nabla^2\mathbf{H}/\mathbf{H})_0 = 2k^2$. It is seen that for low concentrations the maximum space charge is at the center whereas for high concentrations there is a minimum at the center and a maximum part way out to the walls. It may be expected that $(\nabla^2\mathbf{H}/\mathbf{H})_0$ remains between these limits, so that the following bounds may be placed on n_0/s_0:

$$\begin{aligned} (1+\rho)s_0 + \rho/\sigma &\geq (1+\rho)(s_a - s_0)n_0/s_0 \\ &\geq (1-2\rho)s_0 - 2\rho/\sigma; \end{aligned} \tag{37}$$

and one expects the upper bound, which is identical with the constant ratio approximation (13) and (33), to be approached near the free limit, and the lower bound to be approached near the ambipolar limit. The latter statement leads to a surprising result which was first discovered in numerical solutions: when $1/\rho < 2+3/\sigma$ or $s_a < \frac{2}{3}$, that is for a near-isothermal plasma, the lower bound is negative, and therefore $s_0 > s_a$ near the ambipolar limit. As a plasma decays the space-charge parameter s_0, which initially has the value s_a, first increases before decreasing to zero.

In obtaining bounds for n_0/s_0 one must be careful not to divide by a negative number. Considering also the central maximum bound (14), one distinguishes three cases:

(a) $s_a>\frac{2}{3}$, $s_0\leq s_a$

$$\frac{s_0+\rho/\sigma(1+\rho)}{s_a-s_0}\geq\frac{n_0}{s_0}\geq\frac{s_0-(2\rho/\sigma)(1+\sigma s_0)}{(1+\rho)(s_a-s_0)}. \quad (37a)$$

(b) $s_a<\frac{2}{3}$, $s_0<s_a$

$$\frac{s_0+\rho/\sigma(1+\rho)}{s_a-s_0}\geq\frac{n_0}{s_0}\geq\frac{s_0}{1-s_0}. \quad (37b)$$

(c) $s_a<\frac{2}{3}$, $s_0>s_a$

$$\frac{(2\rho/\sigma)(1+\sigma s_0)-s_0}{(1+\rho)(s_0-s_a)}\geq\frac{n_0}{s_0}\geq\frac{s_0}{1-s_0}. \quad (37c)$$

Cases (b) and (c) both apply to the near-isothermal plasma. These bounds will be illustrated in subsequent sections.

VII. THE ACTIVE PLASMA

In an active plasma, $\rho\approx 1/100$, so that the bounds (37a) fall very close to each other and the central ratio n_0/s_0 is well defined. In fact, as $\rho\to 0$, both limits reduce to

$$n_0=s_0^2/1-s_0, \quad (38)$$

and $s_a=1$.

This coalition is best understood by re-writing Eq. (25) in terms of the positive ion concentration $(n+s)$:

$$\rho/\sigma\nabla(n+s)+\mathbf{G}=\mathbf{H}(n+s). \quad (25b)$$

Since $\rho/\sigma=D_+/D_-\approx 10^{-4}$, the first term is negligible over most of the plasma except at densities very near the free diffusion limit. Neglecting this term reduces the order of the equation and therefore reduces the number of arbitrary constants in the solutions. It also reduces the number of boundary conditions to which the solutions may be subjected, and one sees from (25b) that one cannot set both $n_1=0$ and $s_1=0$ at the wall unless the first term is retained. This means that we have neglected the plasma skin whose thickness is of the order $\Delta\xi=\rho/\sigma H_1$.

For an active discharge one therefore seeks solutions of the equations

$$\nabla n+\mathbf{G}=-\sigma\mathbf{H}n, \quad (24)$$

$$\mathbf{G}=\mathbf{H}(n+s), \quad (39)$$

$$\nabla\cdot\mathbf{G}=n, \quad \nabla\cdot\mathbf{H}=s, \quad (26)$$

with the boundary condition $n_1=0$ at the wall.

The free limit of these equations is found as before by setting $H=0$ in (24), and yields the same electron distribution as before [see Eq. (29)]. The space charge is then found by neglecting n in (39) and yields

$$\mathbf{H}\nabla\cdot\mathbf{H}=\mathbf{G}, \quad (40)$$

which is very different from (29). In the case of parallel planes where the electron free limit is $n=n_0\cos\xi$, equation (40) yields $s=(\sqrt{n_0})\cos(\xi/2)$. This change in the limiting form comes from the neglect of the high-order term in (25b). In any actual case ρ/σ is small but not zero. The "limit" obtained above is an intermediate state holding only so long as the ion-mobility term, $H(n+s)$, is larger than the ion-diffusion term $\rho\nabla(n+s)/\sigma$. As the field gets yet smaller, the ion distribution undergoes a second transition to the true free limit given by (29). This low-density change in the ion distribution does not affect the electrons, which are already controlled by diffusion, and therefore does not affect the ionization frequency. It is of no importance for our problem.

a. Analytic Approximation

A good approximation for the active plasma can be obtained by separating it into an interior region, $0<\xi<\xi_p$, and a sheath, $\xi_p<\xi<\xi_1$; at ξ_p, the two regions are joined. The method is illustrated for the case of parallel planes.

The matching point ξ_p is chosen sufficiently far out from the center so that the current $G\approx G_1$ throughout the sheath; it is sufficiently accurate to choose

$$G_1=n_0/k, \quad (41)$$

the value given by the constant ratio approximation. It is further assumed that $n\ll s$ throughout most of the sheath so that (39) becomes $G_1=Hs$. This yields

$$s=G_1^{\frac{1}{2}}[2(\xi-\xi_0)]^{-\frac{1}{2}}, \quad (42)$$

$$H=[2G_1(\xi-\xi_0)]^{\frac{1}{2}}, \quad (43)$$

for $\xi>\xi_p$; ξ_0 is a constant of integration. It is convenient to introduce the independent variable

$$v=\int_{\xi_0}^{\xi}\sigma H d\xi=2\sigma(2G_1)^{\frac{1}{2}}(\xi-\xi_0)^{\frac{3}{2}}/3=\sigma H^3/3G_1 \quad (44)$$

in the sheath; $v=V\mu_-/D_-=eV/k_0T_-$, where V is the potential difference measured from x_0. Equation (44) yields the standard high-pressure sheath,[3] but it will not be joined to the plasma at its origin ξ_0. Using v as the independent variable, Eq. (24) becomes

$$dn/dv+n=-(G_1^2/3\sigma^2v)^{\frac{1}{3}},$$

$$n=(G_1^2/3\sigma^2)^{\frac{1}{3}}e^{-v}\int_v^{v_1}y^{-\frac{1}{3}}e^y dy, \quad (45)$$

for $v>v_p$; $v=v_p$ at $\xi=\xi_p$, and $v=v_1$ at $\xi=\xi_1$.

In the interior region, an approximation better than that given by the constant ratio approximation must be made. It may readily be shown that at the center

$$\left[\frac{1}{s}\frac{d^2s}{d\xi^2}\right]_0=2K^2=\frac{(3s_0-1)k^2}{4-3s_0}. \quad (46)$$

[3] J. D. Cobine, *Gaseous Conductors* (McGraw-Hill Book Company, Inc., New York, 1941), p. 129, Eq. (6.27).

Thus s has a maximum at the center for $s_0<\frac{1}{3}$, and a minimum for $s_0>\frac{1}{3}$, and we choose functions for s satisfying (46) which reduce to the correct ones at the free and ambipolar limits. Considering the intermediate limit of the ions defined by Eq. (40), we choose, in the range $0\leq s_0\leq\frac{1}{3}$,

$$s=s_0\cos\sqrt{2}K\xi, \tag{47}$$

$$H=(s_0\sin\sqrt{2}K\xi)/\sqrt{2}K, \tag{48}$$

where by K we mean $|K|$ throughout. In the range $\frac{1}{3}\leq s_0\leq 1$, we choose

$$s=s_0\sec^2(K\xi), \tag{47a}$$

$$H=s_0\tan(K\xi)/K. \tag{48a}$$

The form of n for $\xi<\xi_p$ is obtained from (24b), but the right-hand side is not negligible in the region $\xi\approx\xi_p$. A reasonable approximation results if it is set equal to n times a power series, and the first term ($\sim\xi^2$) only is retained. By taking second derivatives at $\xi=0$, one finds that, for parallel planes,

$$d^2n/d\theta^2+[1-A\theta^2]n=0, \tag{49}$$

TABLE I. Quantities used in obtaining the free ambipolar transition for an active plasma between parallel planes.

s_0	n_0	$\lvert K/k\rvert$	$\lvert K\xi_p\rvert$	$k\xi_p$	$k\xi_0$	$v_pk^2/\sigma s_0$	$k\xi_1$[a]
0	0	$1/\sqrt{8}$	$\pi/\sqrt{32}$	$\pi/2$	$\pi/2-1$	$\sqrt{8}/3$	$\pi/2$
0.05	0.002632	0.3323	0.5038	1.516	0.5971	0.8526	1.996
0.10	0.01111	0.3076	0.4639	1.508	0.6235	0.8263	2.241
0.20	0.0500	0.2425	0.3642	1.502	0.6773	0.7902	2.470
0.333	0.1666	0	0	1.500	0.750	0.750	2.621
0.50	0.5000	0.3162	0.4670	1.477	0.8412	0.6757	2.676
0.60	0.9000	0.4264	0.6169	1.447	0.8933	0.6137	2.676
0.70	1.633	0.5381	0.7579	1.408	0.9446	0.5440	2.621
0.80	3.200	0.6614	0.9031	1.365	0.9979	0.4700	2.513
0.85	4.817	0.7311	0.9828	1.344	1.029	0.4316	2.432
0.90	8.100	0.8086	1.073	1.327	1.070	0.3937	2.321
0.94	14.73	0.8782	1.162	1.324	1.120	0.3639	2.199
0.96	23.04	0.9161	1.219	1.330	1.154	0.3500	2.111
0.98	48.02	0.9566	1.295	1.354	1.217	0.3373	1.980
0.99	98.01	0.9779	1.354	1.384	1.277	0.3324	1.880
1	∞	1	$\pi/2$	$\pi/2$	$\pi/2$	$\frac{1}{3}$	$\pi/2$

[a] For $\sigma=32$ only.

where

$$A=9\sigma s_0(1-s_0)/2k^2(4-3s_0), \tag{50}$$

$$\theta=k\xi. \tag{51}$$

Equation (49) yields Hermite functions with $n=n_0$ and $dn/d\theta=0$ at $\theta=0$. Since $A=0$ for $s_0=0$ or 1, (49) reduces to the constant ratio approximation at both limits.

The three unknowns ξ_p, ξ_0, and ξ_1 are determined by matching s, H, and n at ξ_p. This eliminates the discontinuities in both s and n which exist in the usual joining method. Matching sH and H/s from (42), (43), (47), or (47a), (48) or (48a) gives, after elimination of G_1 and n_0,

$$\sin2\sqrt{2}K\xi_p=2\sqrt{2}K[k(1-s_0)]^{-1}, \tag{52}$$

$$K\xi_p-K\xi_0=(\tan\sqrt{2}K\xi_p)/2\sqrt{2}; \tag{53}$$

$s_0\leq\frac{1}{3}$

$$\tan K\xi_p\sec^2K\xi_p=K[k(1-s_0)]^{-1}, \tag{52a}$$

$$K\xi_p-K\xi_0=(\sin2K\xi_p)/4. \tag{53a}$$

$s_0\geq\frac{1}{3}$

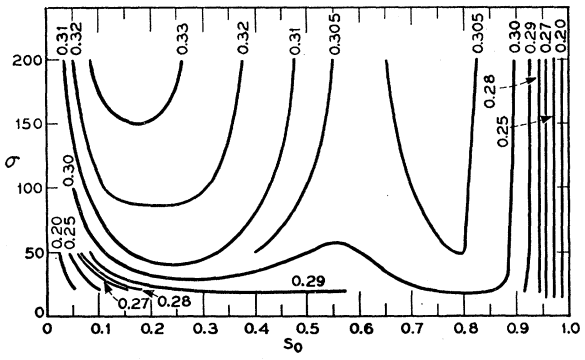

FIG. 1. Contours of constant n_p/n_0 on the s_0, σ plane, as used in Eq. (54).

By matching n

$$\sigma H_pk(n_p/n_0)=v_p^{\frac{1}{3}}e^{-v_p}\int_{v_p}^{v_1}y^{-\frac{1}{3}}e^ydy, \tag{54}$$

where H_p is obtained from Eq. (43), (48), or (48a). The quantities n_0, $|K/k|$, $|K\xi_p|$, $k\xi_p$, $k\xi_0$, and $v_pk^2/\sigma s_0$ are functions only of s_0 and are given in Table I. The ratio n_p/n_0 is a function of s_0 and, to a lesser extent, of σ, and is determined from the solution of Eq. (49); the ratio is plotted in Fig. 1. For $v>0.1$; the function $e^{-v}\int_0^v y^{-\frac{1}{3}}e^ydy$ is nearly constant and is tabulated in Table II. For $v<0.1$, the integral is readily determined from a series expansion.

Equation (54) determines v_1, hence ξ_1, and from the definitions of v, G_1, and n_0,

$$k\xi_1-k\xi_0=[9v_1^2k^4(1-s_0)/8\sigma^2s_0^2]^{\frac{1}{3}}. \tag{55}$$

$k\xi_1$ is a function of s_0, and rather weakly, of σ. It is shown in Table I, computed for the value $\sigma=32$; however, it is believed that the value of $k\xi_1$ *vs* s_0 will be much the same for all σ.

One can now compute D_s and ν from (28) and (9), the real charge densities, and other quantities. For example, $E_1\Lambda\mu_-/D_-=\sigma H_1(D_s/D_-)^{\frac{1}{2}}$ is proportional to the space-charge field at the wall, and H_1 is calculated

TABLE II. The function $F(v)=e^{-v}\int_0^v y^{-\frac{1}{3}}e^ydy$.

v	$F(v)$
0	0
0.10	0.305
0.20	0.456
0.30	0.516
0.40	0.645
0.50	0.705
0.60	0.753
0.80	0.823
1.0	0.864
1.5	0.889
2.0	0.863
3.0	0.780
4.0	0.701
5.0	0.639
6.0	0.592
7.0	0.555
∞	0

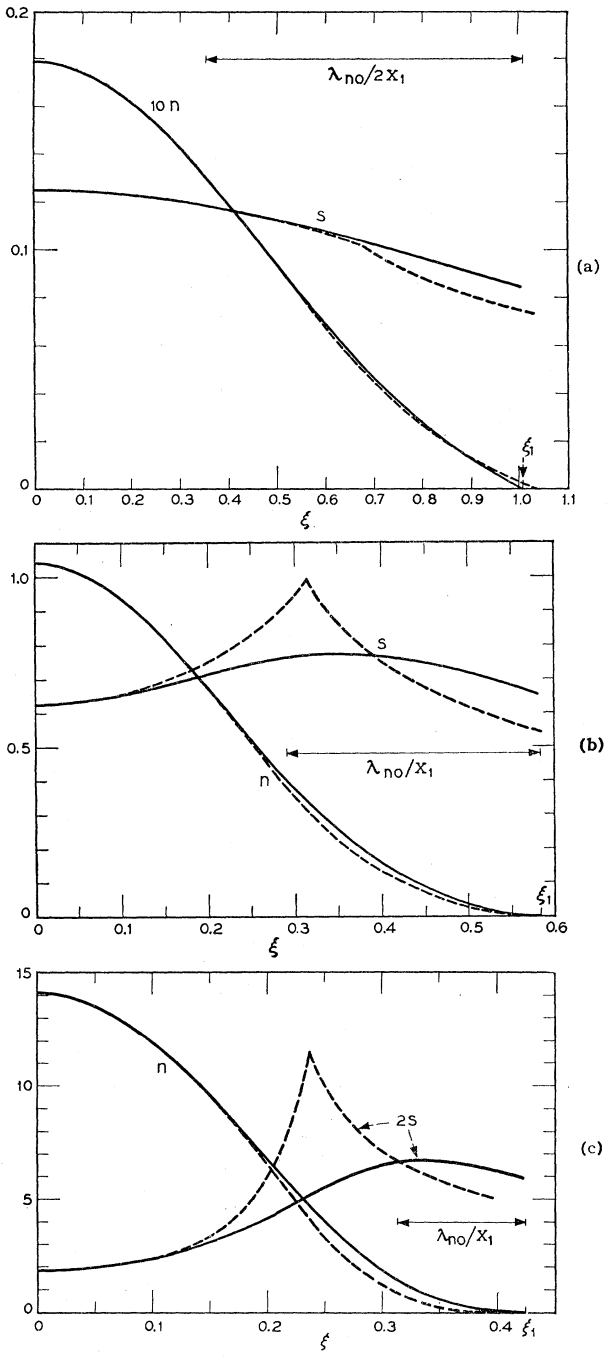

FIG. 2. Machine (———) and analytic (– – – –) distributions of n and s *vs* distance parameter ξ for an active discharge between parallel planes, with $\rho=0$, $\sigma=32$. The center is at $\xi=0$, and the wall at $\xi=\xi_1$. (a) Low density, $s_0=0.125$, $n_0=0.01786$; (b) Intermediate density, $s_0=0.625$, $n_0=1.041$; (c) Near-ambipolar, $s_0=0.9375$, $n_0=14.06$.

from Eq. (44). Similarly $V_1\mu_-/D_-=-\int_0^{\xi_1}\sigma H d\xi$ is proportional to the wall potential V_1 relative to the center, so that

$$V_1=-(D_-/\mu_-)\left[\int_0^{\xi_p}\sigma H d\xi+v_1-v_p\right]. \tag{56}$$

Whether one defines the sheath as originating at ξ_p or ξ_0 (as has been customary) is a matter of convenience. Choosing ξ_p results in a sheath which first expands as s_0 decreases from s_a, then shrinks to zero at the free limit. With this choice, the sheath potential becomes

$$V_{sh}=D_-(v_1-v_p)/\mu_-. \tag{57}$$

(b) Approximation Near the Ambipolar Limit

The ambipolar limit is approached as $s_0\to 1$, and asymptotic expressions can be given for the quantities required by the theory. These are obtained by setting $K=k$, $\sin(k\xi_p)=1$, $\cos(k\xi_p)=\sin(\pi/2-k\xi_p)=\pi/2-k\xi_p$, and are as follows:

$$\pi/2-k\xi_p=(1-s_0)^{\frac{1}{2}}; \tag{52b}$$

$$k(\xi_p-\xi_0)=(1-s_0)^{\frac{1}{2}}/2; \tag{53b}$$

$$\sigma s_0=v_p^{\frac{1}{2}}e^{-v_p}\int_{v_p}^{v_1}y^{-\frac{1}{2}}e^y dy; \tag{54a}$$

$$k(\xi_1-\xi_0)=(1-s_0)^{\frac{1}{2}}(v_1/v_p)^{\frac{1}{2}}. \tag{55a}$$

Since

$$v_p=\sigma s_0/3k^2\approx\tfrac{1}{3}, \tag{44a}$$

Eq. (54a) may be further approximated by

$$v_1\approx 1.08\ln(2.20\sigma s_0). \tag{54b}$$

As $n_0=s_0^2/(1-s_0)$, it is seen that the sheath thickness varies as $n_0^{-\frac{1}{2}}$ or $N_0^{-\frac{1}{2}}$ and that the space-charge field E_1 at the wall varies as $N_0^{\frac{1}{2}}$. The analog to the Langmuir sheath is given by the thickness $\xi_1-\xi_0$. As our interior solution is much better than the conventional one, we have joined at ξ_p instead of at ξ_0.

In the ambipolar limit, our sheath potential becomes

$$V_{sh}=1.08(D_-/\mu_-)\ln(2.20\mu_-/\mu_+)-D_-/3\mu_-; \tag{57a}$$

the last term is a small correction arising from the choice of ξ_p, rather than ξ_0, as the sheath edge. Equation (57a) differs from Langmuir's expression[4]

$$V_{sh}=(k_0T_-/e)\ln(T_-m_+/T_+m_-), \tag{58}$$

where m_+ and m_- are the ionic and electronic masses, principally in the nature of the logarithmic term. Our relation (57a) is derived on the assumption that the mean free path is small compared to the sheath thickness, so that the mobilities, hence the ratio of electron to ion drift velocities, are involved. Equation (58) applies when the mean free path is long and the charges fall freely; the logarithmic term is essentially the ratio of the random velocities. As N_0 increases and the sheath gets thinner according to (55a) one eventually reaches a point where the sheath is thin compared to the mean free path and then one must use Eq. (58). A transition between the two types of sheath, however, may not be observed in practice, for sheath voltages calculated by the two relations do not differ markedly; it is proper to

[4] I. Langmuir, Phys. Rev. **33**, 969 (1929).

compare them after omitting the last term of (57a). For hydrogen, $\sigma\approx 32$, $\rho\approx 100$; Eq. (57a) gives $V_{sh}\mu_-/D_- = 4.6$; and (58) gives 6.4. For oxygen, $\sigma\approx 400$, $\rho\approx 70$; both (57a) and (58) give $V_{sh}\mu_-/D_-\approx 7.3$.

Extension of the near-ambipolar solution to a cylindrical or spherical geometry is simple. Since the sheath is thin, its form is unaltered, and only the matching at ξ_p must be adjusted; it is necessary only to replace the form of the constant ratio approximation with the one applicable to the geometry in question.

(c) Machine Solutions

For an active discharge in hydrogen, the appropriate parameters are $\rho\approx 1/100$, $\sigma\approx 32$. Thus the case $\rho=0$, $\sigma=32$ for a cavity consisting of infinite parallel planes was solved on the Mark IV computer at Harvard University. Central concentrations s_0 were chosen arbitrarily, and the appropriate concentrations n_0 were

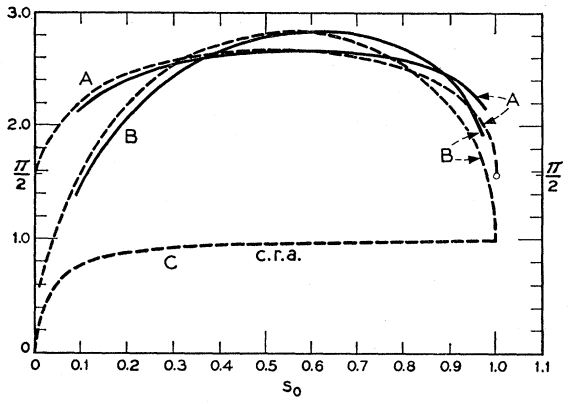

FIG. 3. Machine (———) and analytic (- - - -) solutions of the quantities $k\xi_1$ (A) and s_0D_s/D_a (B) *vs* s_0 for an active discharge between parallel planes, with $\rho=0$, $\sigma=32$. The quantity s_0D_s/D_a is proportional to the true central space charge, and it is noted that the central space charge exceeds the ambipolar value through most of the transition. The value of s_0D_s/D_a obtained from the constant ratio approximation (c.r.a.) (C) is also shown.

computed from Eq. (38). The equations were integrated from the center outward to the point ξ_1 where $n=0$.

Figure 2(a) shows both the machine solutions and the analytic approximation for n and s *vs* ξ with $s_0=0.125$, $n_0=0.01786$. Figure 2(b) shows n and s for $s_0=0.625$, $n_0=1.041$; such densities lie about mid-way through the transition region. Figure 2(c) shows n and s for $s_0=0.9375$, $n_0=14.06$, approaching the ambipolar region. These figures illustrate the change in shape of $s(\xi)$ with increasing density and the development of the bell-shaped distribution of n indicative of sheath formation. The length λ_{n0} is the Debye length corresponding to the central electron density. The ratio $\lambda_{n0}/x_1=(\sigma n_0\xi_1^2)^{-\frac{1}{2}}$ is marked off on Figs. 2(b) and (c), and the ratio $\lambda_{n0}/2x_1$ is marked on Fig. 2(a).

While the distribution of s is rather crudely approximated by the theory, the end point ξ_1 and the various

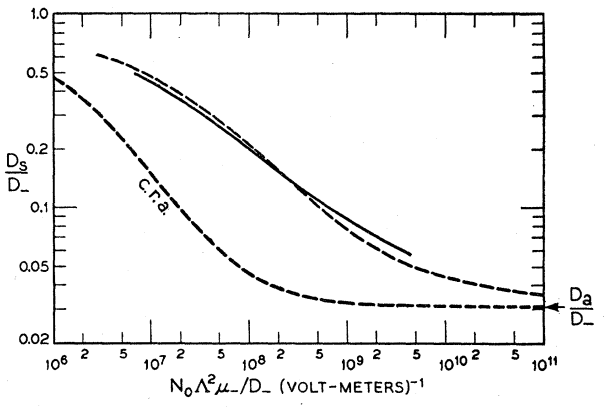

FIG. 4. Machine (———) and analytic (- - - -) solutions of the effective diffusion coefficient D_s/D_- *vs* central electron density $N_0\Lambda^2\mu_-/D_-$ for an active discharge between parallel planes, with $\rho=0$, $\sigma=32$. The constant ratio approximation is also shown.

integrals over n and s are reasonably accurate. Curves A of Fig. 3 show the quantity $k\xi_1$ *vs* s_0 for both the machine and analytic solutions, the latter also being tabulated in Table I. The c.r.a. of course would give $k\xi_1=\pi/2$, and the difference is a rough measure of the sheath thickness. The true central space charge,

$$(P-N)_0e=\epsilon_0\nu s_0/\mu_+=s_0D_s\epsilon_0/\mu_+\Lambda^2, \qquad (59)$$

as distinct from the central space charge parameter s_0, is measured by the product s_0D_s. This goes above its ambipolar value, and this peculiarity is shown by plotting s_0D_s/D_a *vs* s_0 in curves B of Fig. 3. The constant ratio approximation value of s_0D_s/D_a is shown by curve C and makes it evident that although this approximation goes to the ambipolar limit it does not approach it in the right way.

Figure 4 shows $D_s/D_-=(2\xi_1/\pi)^2$ plotted *vs* $N_0\Lambda^2\mu_-/D_- = \epsilon_0D_sn_0/eD_-$ (volt-meter)$^{-1}$, which is proportional to

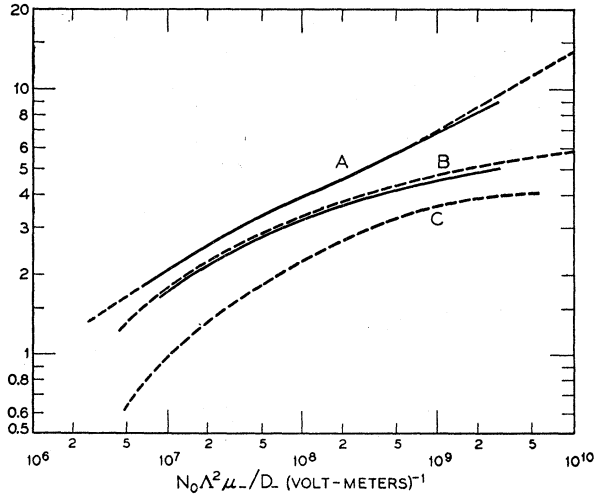

FIG. 5. Machine (———) and analytic (- - - -) solutions of wall field $E_1\Lambda\mu_-/D_-$ (A), wall potential $-V_1\mu_-/D_-$ (B), and sheath potential $V_{sh}\mu_-/D_-$ (C) *vs* central electron density $N_0\Lambda^2\mu_-/D_-$ for an active discharge between parallel planes. $\rho=0$, $\sigma=32$.

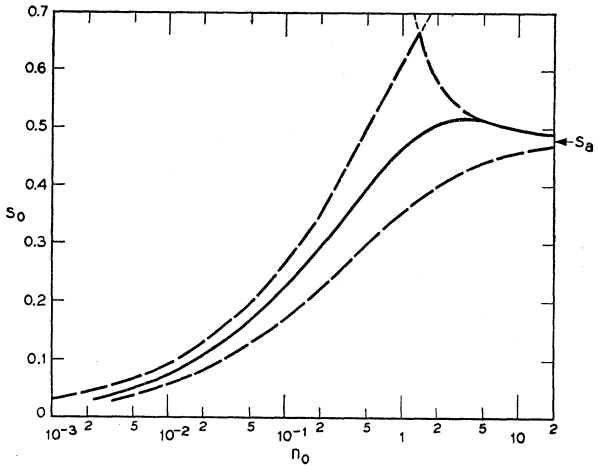

Fig. 6. Machine solution (———) and analytic limits (– – – –) of space-charge parameter s_0 *vs* electron density parameter n_0 for an isothermal plasma between parallel planes with $\sigma=32$. Note that s_0 rises above $s_a=0.484$ through part of the transition region.

the true central electron density; for comparison, the constant ratio approximation (34) is also shown.

The quantities $E_1\Lambda\mu_-/D_-$ and $-V_1\mu_-/D_-$, for both machine and analytic solutions, are plotted in Fig. 5 *vs* $N_0\Lambda^2\mu_-/D_-$. $V_{sh}\mu_-/D_-$ as obtained from the analytic solution is also shown. Since it is the development of the space-charge voltage that inhibits the electron flow and brings about the free ambipolar transition, it is not surprising to discover that the wall potential is substantially in excess of the average electron energy through most of the transition.

The transition itself takes place over several orders of magnitude. If, for example, $D_-/\mu_-=2$ volts and $\Lambda=1$ cm, then $D_s/D_-\approx 0.5$ at $N_0=2\times10^4/\text{cm}^3$; and, even at this low density, the net central space charge is about equal to that obtained at the ambipolar limit.

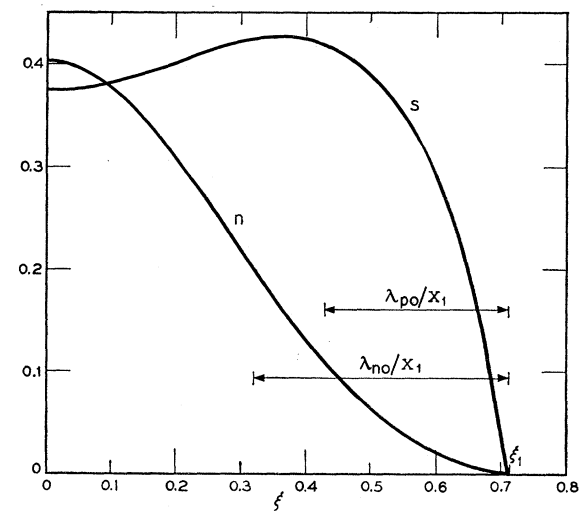

Fig. 7. Machine solutions of n and s *vs* ξ for an isothermal plasma between parallel planes with $\sigma=32$; $s_0=0.375$, $n_0=0.4031$.

The limit itself, however, is not closely approached below $N_0\approx10^9/\text{cm}^3$.

VIII. THE ISOTHERMAL PLASMA

The problem of the isothermal plasma in an infinite parallel plane cavity was solved on the Whirlwind computer at the Massachusetts Institute of Technology for the case $\rho=1$, $\sigma=32$. Since the effects of ion diffusion are not negligible, n_0 is not directly determined in terms of s_0. Thus central concentrations (n_0, s_0) were chosen arbitrarily and the equations integrated from the center outward. Solutions for which n and s did not vanish at the same coordinate were rejected and the solution repeated for a different value of n_0. Appropriate pairs (n_0, s_0) were found and for these the entire solution was plotted, and the value of ξ_1 recorded. Figure 6 shows s_0 as a function of n_0 from the machine solutions and the two limits (37b) and (37c) and illustrates the departure from these bounds. It shows

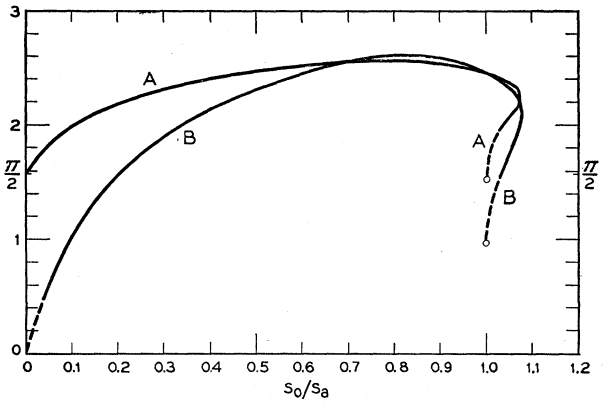

Fig. 8. Machine solutions of the quantities $k\xi_1$ (A) and s_0D_s/s_aD_a (B) *vs* s_0/s_a for an isothermal discharge between parallel planes, with $\sigma=32$.

s_0 passing above its ambipolar value s_a. Figure 7 shows the machine solutions of n and s *vs* ξ with $s_0=0.375$, $n_0=0.4031$, about midway in the transition. The ratios λ_{n0}/x_1 and $\lambda_{p0}/x_1=[\sigma(n+s)_0\xi_1^2/\rho]^{-\frac{1}{2}}$ are marked on the figure. The spatial distributions are generally similar to those of Figs. 2(a)–(c) except in the following details: (i) s drops to zero at $\xi=\xi_1$, but still shows a maximum part way out for the higher values of s_0; (ii) since the ions diffuse freely at the free limit, $s=s_0\cos\xi$ at the free limit rather than $s_0\cos\xi/2$ as was the case for $\rho=0$; (iii) at the ambipolar limit $s_a=0.484$ rather than unity, and the maximum value of s_0 in the transition was 0.519.

Figure 8 shows the quantities $k\xi_1$ and s_0D_s/s_aD_a plotted *vs* s_0/s_a and illustrates the peculiarities both in the true central space charge and in s_0. Comparison with Fig. 3 shows that the maximum sheath thickness is about the same for both $\rho=0$ and $\rho=1$.

Figure 9 shows D_s/D_- *vs* $N_0\Lambda^2\mu/D$. For comparison, the constant ratio approximation (34) is also shown,

using Eq. (33) to determine n_0 as a function of s_0. The figure shows that $|dD_s/dN_0| \ll D_s/N_0$; thus a thermal plasma initially situated on the curve will decay in a quasi-equilibrium fashion closelyf ollowing the curve.

Finally, $E_1\Lambda\mu/D$ and $V_1\mu/D$ are plotted in Fig. 10 *vs* $N_0\Lambda^2\mu/D$.

Inasmuch as most of the fundamental processes are the same for $\rho=0$ and $\rho=1$, it is not surprising that the results in the two cases are quite similar. It has not been possible, however, to obtain satisfactory analytic expressions for the case $\rho=1$, and the mathematical difficulty arises because perturbations at the wall are transmitted by the ions much further into the interior of the isothermal than into the active plasma. For the same reason, an experimental probe will disturb an isothermal plasma more deeply than an active one. As a result of these difficulties, it is possible to solve the isothermal case only by machine methods.

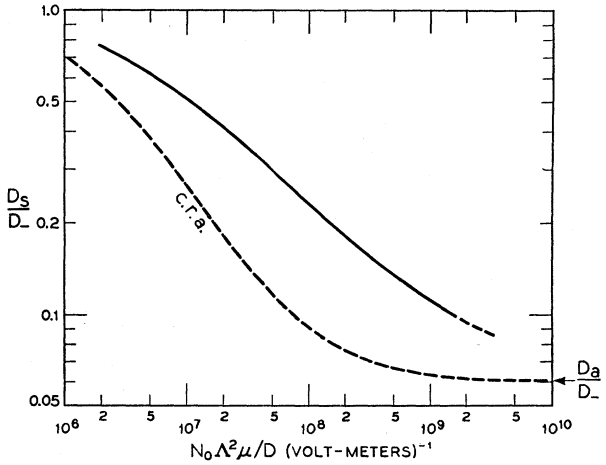

FIG. 9. The effective diffusion coefficient D_s/D_- *vs* central electron density $N_0\Lambda^2\mu/D$ for an isothermal discharge between parallel planes, with $\sigma=32$. The c.r.a. is also shown.

IX. CONCLUSION

A very simple approximation termed the constant ratio approximation (c.r.a.), has been found. Although it goes to the correct free and ambipolar limits. it is shown to be in error by a factor which may be of the order 3. A good second approximation has been found for the case of an active plasma ($T_+/T_-=\rho \ll 1$). This is obtained by joining a sheath to interior solutions which consist, for the case of parallel planes, of Hermite and trigonometric functions. The joining is done so that

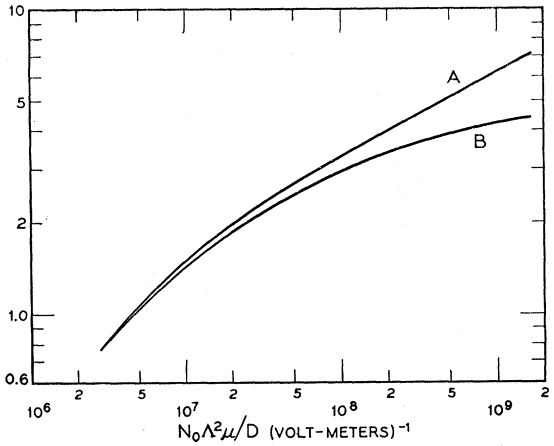

FIG. 10. Wall field $E_1\Lambda\mu/D$ (A) and wall potential $-V_1\mu/D$ (B) *vs* central electron density $N_0\Lambda^2\mu/D$ for an isothermal discharge between parallel planes, with $\sigma=32$.

electron and ion densities, field, and current are all continuous. From this solution the development of a sheath, with increasing plasma density, can be followed. All quantities are compared with an exact machine solution. An effective diffusion coefficient D_s is calculated, from which the ionization frequency $\nu=D_s/\Lambda^2$ can be calculated. The free-ambipolar transition takes place over many orders of magnitude of electron density, and the ambipolar limit is approached very gradually.

The method used for the active plasma fails for the isothermal plasma ($\rho=1$) because the boundary conditions react on the central ratio P_0/N_0 of ion to electron concentrations. This has experimental implications in the use of probes. Machine solutions have been obtained here also and show that aside from the central ratio the transition is quite similar to that for an active plasma. It is shown that the relative change of D_s is slow compared to that of the concentration N_0 and that therefore the solutions obtained may be applied to a decaying plasma for which $\partial N/\partial t=-ND_s/\Lambda^2$.

ACKNOWLEDGMENT

We are greatly indebted to Mr. Robert Minnick of Harvard University who coded these problems for machine computation and supervised their solutions and to Mr. J. T. Gilmore of the Whirlwind Project at the Massachusetts Institute of Technology who operated this machine.